Modeling Frequency Response of Photoacoustic Cells using FEM for Determination of N-heptane Contamination in Air: Experimental Validation

Lars DUGGEN, Mihaela ALBU, Morten WILLATZEN, and Horst-Günter RUBAHN
NanoSYD, Mads Clausen Institute, University of Southern Denmark
Alsion 2, DK-6400 Sønderborg, Denmark

ABSTRACT

We briefly present the basic principle of the photoacoustic effect in gases. We present the equations and boundary conditions governing the acoustic field generated by the absorption of a modulated laser beam. We solve these equations using Finite Element Methods and compare the results with experiment. We find that apparently there are effects not taken into account in the classic acoustic theory as we find a larger damping than theory predicts. However, we see that these effects have significant negative influence on the quality factor of the cell and thereby the performance limit.

Keywords: Photoacoustic effect, acoustic damping, FEM, n-heptane contamination.

1. INTRODUCTION

The photoacoustic effect was discovered by Alexander Graham Bell in 1880 and has drawn considerable scientific and engineering attention after the 1960's in connection with the invention and availability of lasers [1]. Its broad range of applications include photoacoustic spectroscopy, with the advantage of applicability to solids (also soft tissue) as well as fluids. This diversity makes it feasible for non-invasive medical applications, biological, and environmental applications [2, 3, 4].
Here we focus on the measurement of n-heptane concentrations in air, which is a model system for an application towards measurement of oil contaminations in air. For experimental convenience we chose to conduct experiments on n-heptane as it shares many critical properties (as optical absorption spectrum) with oil without having the drawback of sticking to the surfaces. Thus, compared to using oil, the photoacoustic cell is easy to clean after experiments.
Since the generated acoustic signal might be rather small, it is convenient to make use of acoustic resonance as a natural amplifier of the signal. In order to design the cell according to desired requirements such as resonance frequency (such that it fits to the microphone and laser driver specifications), mathematical modeling is a crucial tool. Mathematical models for the photoacoustic effect have been developed since the middle of the 1970's, started by a theoretical description of the photoacoustic effect with solids [5, 6, 7]. Regarding gas-photoacoustics there exist several works considering the theory behind [8], specifically loss mechanisms [7, 9, 1]. However, many of these works are limited to rather simple geometries, being a limiting factor for the effective design of a photoacoustic cell. There have also been works concerning the simulation of photoacoustic cells using Finite Element Methods [10, 11, 12], however there still are problems modeling the loss mechanisms correctly.
Despite using a rather simple geometry, in principle covered by the existing theory, we will present a slightly more general model and solve it using the Finite Element Method (FEM), comparing it with the experiment in order to find a reliable method to model more complex photoacoustic cells using FEM. Furthermore we will discuss experimental results and analysis of these.

2. THEORY

The basic theory behind the photoacoustic effect can briefly be described as follows, focusing on the photoacoustic effect in gas. The contaminated air (i.e. synthetic air and n-heptane) is lead into a closed cell as depicted in Figure 1. Then a laser beam is sent through the cell. The wavelength of the laser is tuned such that it fits to a contaminant absorption peak. When being absorbed, molecular rotational/vibrational states are excited and these states are subsequently relaxed by molecular collisions, essentially heating up the gas in the small volume around the particular molecule that absorbed laser light. Finally the laser intensity is modulated (in this case sinusoidally) and the heating will cause thermal and pressure waves throughout the gas mixture. The pressure wave is then measured by a microphone. The amplitude of the acoustic signal depends linearly on the strength of the laser and the concentration of the contaminant (up to possible saturation limits at very low concentrations).

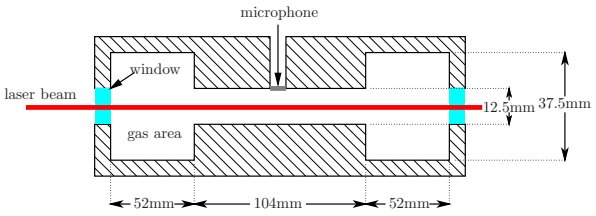

Figure 1: Cross section of the cylindrical photoacoustic cell used. The cell is made of stainless steel, gold coated while the windows are made of BK7 glass.

The photoacoustic effect can be described theoretically by fundamental thermodynamic laws regarding the absorption of the laser light as heat energy input [13, 14]. Manipulations as well as assumptions about a small viscosity and small heat transfer coefficient (such that only first order terms need to be accounted for) together with small temperature and pressure deviations, yields the Helmholtz equation in acoustic pressure p reading

$$\nabla^2 p + k^2 p = -i\omega \frac{P_0 \gamma \varepsilon}{T_0 C_p c^2}. \quad (1)$$

Here it is assumed that the heat input function ε is a monofrequency input such that general time dependence can be obtained by a Fourier transform of the time dependent input. Here, p denotes the acoustic pressure (i.e. pressure change generated by the laser), C_p is the heat capacity at constant pressure, γ denotes the ratio of specific heats, c is the speed of sound, and P_0, T_0 are the equilibrium pressure and temperature, respectively. The value of k is the wavenumber ω/c, where we pick the lossless wavenumber as the classical bulk loss effects are negligible [11].
The boundary condition in radial coordinates reads [11]

$$\left.\frac{\partial p}{\partial r}\right| r_R = i\omega\rho_0 \left[\frac{1}{z} - \frac{i+1}{\rho_0 c}\left((\gamma-1)\frac{J_1\left(\sqrt{\frac{i\omega}{l_h c}}R\right)}{J_0\left(\sqrt{\frac{i\omega}{l_h c}}R\right)}\sqrt{\frac{l_h\omega}{2c}} + \frac{k_t^2 c^2}{\omega^2}\frac{J_1\left(\sqrt{\frac{i\omega}{l_v c}}R\right)}{J_0\left(\sqrt{\frac{i\omega}{l_v c}}R\right)}\sqrt{\frac{l_v\omega}{2c}}\right)\right] p, \quad (2)$$

where z, ρ_0, J_n, k_t denote acoustic impedance of the wall material, equilibrium mass density, n-th order Bessel function, and transverse wavenumber (see discussion in [11, 13]), respectively. Furthermore l_h, l_v denote thermal and viscous loss terms given by

$$l_h = \frac{K}{\rho_0 C_p c}, \quad (3)$$

$$l_v = \frac{\mu}{\rho_0 c}, \quad (4)$$

where K is the heat conductivity and μ is the bulk viscosity.
This equation is solved for the given geometry using Comsol Multiphysics 3.5® as two-dimensional problem with the Cartesian differential operators transformed into their polar counterparts.
We solve both the case where all losses are taken exactly as above (sim. w/o fit) and the case where we fit the loss parameters in this simulation to experimental results (sim. with fit). Finally the amplitude of the simulation with fit is scaled such that it corresponds to the experimental amplitude. The ratio between the two simulated results is kept constant in order to compare the two simulations. This indicates the real quality of the cell compared to the theoretical (i.e. ideal) quality of the cell of given dimensions.

3. EXPERIMENTAL SETUP

The cell used is depicted in Figure 1. The photoacoustic signal is detected by a fibre optic microphone "Optimic 4110 FA" from Optoacoustics. This ultra low noise microphone is designed for monitoring very weak sound signals in selected bandwidths and has a sensitivity of 5 V/Pa. It has a resonance frequency of 1.65 kHz and a -3 dB conformity from 1.40 to 1.80 kHz. The electrical signal is furthermore filtered and amplified with a "Kemo BenchMaster" 8.41 filter/amplifier unit with an adjustable band pass filter (8 pole Butterworth filter -48 dB/octave) from Kemo Limited. We have set the passband to be from 1350 to 1980 Hz. The refurbished signal is connected to a lock-in amplifier (model SR 830 from Stanford Research Systems) to extract the correlated amount from the signal. A calibrated commercial instrument, "1314 Photoacoustic Multi-gas Monitor" from Innova Air Tech Instrumennts, was used as a reference to monitor the contamination level of n-heptane. Each acoustic frequency is excited and measured for three seconds.
The contaminated gas samples are prepared by initially introducing a small amount of n-heptane (typically around 20 ppm) into synthetic air and measuring the concentration by the reference device. Subsequently, after each measurement series covering the acoustic frequencies of interest, this sample is diluted to half of the previous concentration, thus giving a reliable concentration.
The measurements are then fitted to the following function, based on the response of the damped oscillator, i.e. on the same fundamental principle resulting in damped harmonic vibrations:

$$p_{fit} = \frac{A}{\sqrt{\omega_s^4 m^2 + \omega_s^2 (R_m^2 - 2sm) + s^2}}, \quad (5)$$

where $\omega_s = 2\pi(f - f_s)$ with f being the acoustic frequency in Hz and f_s is a fitting parameter. Furthermore s, m, and R_m are fitting parameters roughly corresponding to bulk modulus, mass density, and allover damping, respectively. However, these parameters are only fitted once as they represent cell and gas properties which do not change significantly (assuming temperature and pressure are kept almost constant). Finally, for each measurement set the parameter A is fitted, being the indicator of signal strength.
This fitting function has shown to work reasonably well and is quite robust to single signal outliers. Also we have tried several polynomial fitting functions of degrees up to seven. The harmonic fitting function showed to have the least accumulated error $\sum_{n=1}^{n_{meas}} (p_{fit,n} - p_{meas,n})^2$, where $p_{fit,n}$ are the respective pressures obtained by the fitting function at a certain frequency (denoted by index n, i.e. $f = f_0 + n \cdot \Delta f$) and p_{meas} are the corresponding measured pressures, while n_{meas} simply denotes the amount of measured pressures.

4. RESULTS

We have used two different cell designs; one a described above (figure 1) and one as described in [12].
The result for a single concentration measurement obtained by the prototype described in [11] is shown in Figure 2. We have found that, using the simulation with fitted loss parameters, we obtain very good agreement with experiments, indicating the feasibility of this model.

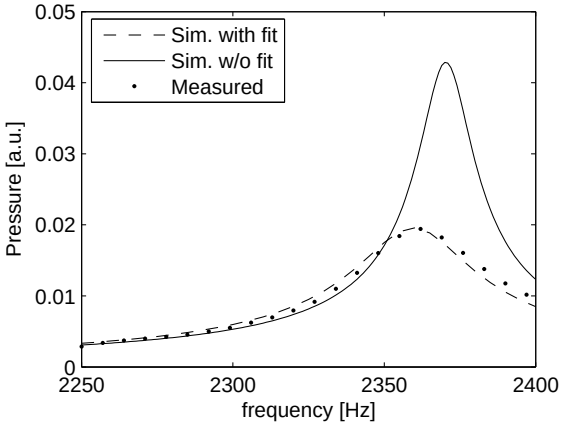

Figure 2: Measured and simulated pressure for a photoacoustic cell of total length 143 mm, a resonator diameter of 15 mm and a buffer diameter of 35 mm [12]

Results for the acoustic signal at a concentration of 14 parts-per-million (ppm), using the cell design described here, are shown in Figure 3.
We find, as before [11], that the damping considered in the boundary condition given above is not sufficient to describe the actual acoustic signal. Note that for the dotted curve we have used standard values for the thermodynamic properties of air only; we have

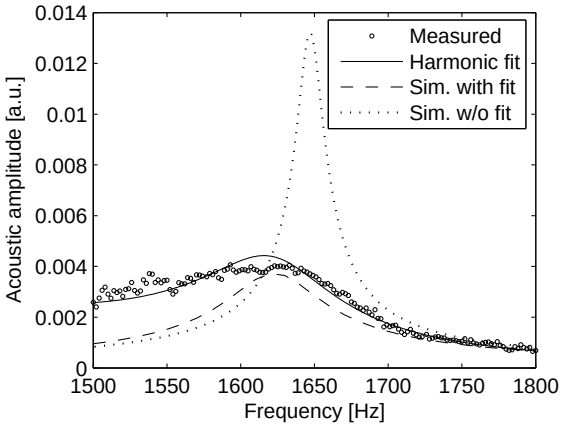

Figure 3: Acoustic signal with n-heptane concentration of 14 ppm at different frequencies

only scaled the amplitude of the curve as the measured signal is also subject to electronic amplification. However, we find that an artificial increase of the boundary effects, obtained by scaling of the l_h and l_v parameters, leads to a better agreement. This is seen as the dashed curve in Figure 3, where we conduct the same simulation with the imaginary terms in equation (2) multiplied by 3.4. Nevertheless, there seem to be some effects in the cell that our model does not capture, as the shape of the simulated response does not fit the measured response very well.

The amplitude of the acoustic signal is shown in Figure 4, where the amplitude is seen to depend on the n-heptane concentration somewhat linearly, although with some deviations. This indicates the importance of a complete understanding of the acoustic effects apparent in the cell in order to find the origin of these deviations and remove them as far as possible in the cell design.

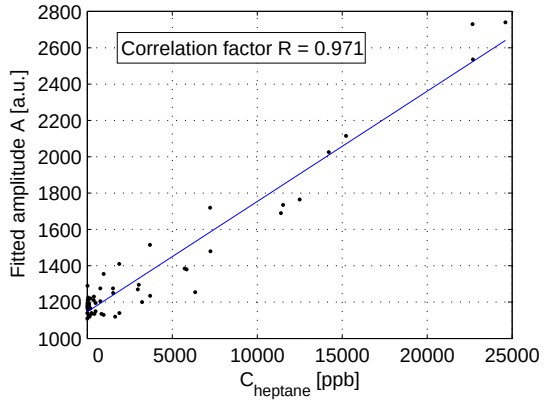

Figure 4: Measured pressure amplitudes at resonance for different n-heptane concentrations, using the cell depicted in Figure 1

5. CONCLUSIONS

We have briefly presented the basics of the photoacoustic effect and have employed the theory to simulate the acoustic behavior of the cell using Finite Element Methods.

We have conducted experiments using synthetic air contaminated with n-heptane and found that a modified version of a damped oscillator resonance is a quite reasonable fitting function, being more stable than high-order polynomials and giving the least accumulated error.

We have found a reasonably good linear behavior of signal strength vs. n-heptane concentration, although there are deviations.

Because of the fact that we obtain quite good agreement with one prototype (Figure 2) and the reasonable agreement only on one edge with the other prototype (Figure 3), we believe it is important to examine the frequency response further, measuring other resonance frequencies as well as changing other parameters and reconsidering details of the model.

6. ACKNOWLEDGMENTS

We gratefully acknowledge the financial support from the Danish National Advanced Technology Foundation.

7. REFERENCES

References

[1] A. Miklos, P. Hess, and Z. Boszoki. Rev. Sci. Instrum., **72**, 1937 (2001).

[2] C. Haish and R. Niessner. Spectroscopy Europe, **14**, 10 (2002).

[3] F. Bijnen, J. Reuss, and F. Harren. Rev. Sci. Instrum., **67**, 2914 (1996).

[4] B. Cox, S. Kara, S. Arridge, and P. Beard. J. Acoust. Soc. Am., **121**, 3453 (2007).

[5] A. Rosencwaig and A. Gersho. Journal of Applied Physics, **47**, 64 (1976).

[6] F. McDonald and G. Wetsel. Journal of Applied Physics, **49**, 2313 (1978).

[7] R. Kamm. Journal of Applied Physics, **47**, 3550 (1976).

[8] G. Diebold and P. Westerveld. J. Acoust. Soc. Am., **84**, 2245 (1988).

[9] J. Mehl and M. Moldover. J. Chem. Phys., **74**, 4062 (1981).

[10] B. Baumann, B. Kost, H. Groninga, and M. Wolff. Rev. Sci. Instrum., **77**, 044901 (2006).

[11] L. Duggen, N. Lopes, M. Willatzen, and H.-G. Rubahn. Intern. Journ. of Thermophys., **32**, 774 (2011).

[12] L. Duggen, R. Frese, and M. Willatzen. Jour. of Phys.: Conf. Series, **214**, 012036 (2010).

[13] P. Morse and K.U.Ingard. *Theoretical Acoustics*. Princeton Univ. Press, Princeton, NJ (1986).

[14] L. Kinsler, A. Frey, A. Coppens, and J. Sanders. *Fundamentals of Acoustics*. Wiley & Sons Inc., Hoboken, NJ (1999).